

# A Simple Power Diode Model with Forward and Reverse Recovery

Cliff L. Ma and P. O. Lauritzen

**Abstract**—The basic diode charge-control model used in SPICE is extended by employing the lumped charge concept of Linvill to derive a set of model equations from simplified device physics. Both forward and reverse recovery phenomena are included as well as emitter recombination. The complete model requires only seven relatively simple equations and three additional device parameters beyond the generic SPICE diode model.

## I. INTRODUCTION

**M**ODELING of the transient behavior of power diodes is extremely important for power electronic circuit simulation. Yet, the diode models widely used in analog circuit simulators such as SPICE do not contain the equations for forward and reverse recovery [1]. Inclusion of these phenomena is critical for the simulation of switching power loss, conducted EMI or any other waveform sensitive effects.

Existing power diode models can be classified as either macrocircuit models [2] or detailed physical models [3]. The macrocircuit models are composed of electrical equivalent circuits which are not directly related to internal physical processes in the device. Thus, they are normally valid for only a narrow range of circuit operating conditions. In contrast, most physical models include equations for drift and diffusion of electrons and holes. They usually contain many mathematical equations and parameters, and are complicated to incorporate into circuit simulators.

The diode model presented here is a simplified physical model for a high voltage p-i-n structure operating in high level injection as is typical for most power diodes. The model is an extension of the basic charge-control diode model using the lumped charge concept of Linvill [4]. The equations for both forward and reverse recovery as well as emitter recombination are derived from simplified semiconductor charge transport equations.

## II. MODEL DESCRIPTION AND DERIVATION

### A. Reverse Recovery

Reverse recovery occurs when a forward conducting diode is turned off rapidly, and the internally stored charges cause transient reverse current to flow at high reverse voltage. Fig.

Manuscript received July 17, 1991; revised April 22, 1993. This work was supported by the NSF-CDADIC University-Industry Cooperative Center for Design of Analog/Digital Integrated Circuits.

The authors are with the Department of Electrical Engineering, University of Washington, Seattle, WA 98195.

IEEE Log Number 9211703.

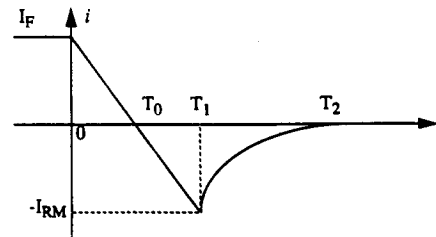


Fig. 1. Turn-off current waveform with an inductive load.

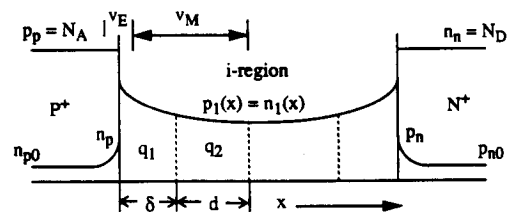


Fig. 2. Charge distribution profile in diode forward conduction.

1 shows a typical reverse recovery current waveform with an inductive load.

Fig. 2 shows the charge distribution in a conducting p-i-n diode under forward conduction corresponding to  $t \leq 0$  on the curve in Fig. 1. The charge distribution in the *i*-region is assigned to four charge storage nodes following the lumped model approach developed by Linvill [4]. Here for simplicity, equal hole and electron mobilities are assumed which makes the charge distributions symmetric and allows the analysis to be simplified to only half of the structure.

The total charge in the left node is  $q_1 = qA\delta p_1$ , and in the adjacent node is  $q_2 = qAdp_2$ , where  $q$  is the unit electron charge,  $A$  is the junction area,  $\delta$  and  $d$  are the widths of the respective regions, and  $p_1$  and  $p_2$  are the average hole concentrations corresponding to  $q_1$  and  $q_2$ . According to the ambipolar diffusion equation, the current  $i_M$  between the two nodes can be expressed as

$$i_M(t) = -2qAD_a \frac{dp}{dx} = \frac{2qAD_a(p_1 - p_2)}{\frac{\delta}{2} + \frac{d}{2}} \quad (1)$$

where  $D_a$  is the ambipolar diffusion constant. When the diode becomes reverse biased, the charge  $q_1$  is exhausted first. Thus once  $q_1$  reaches zero, additional charge is available only by diffusion from the adjacent node containing  $q_2$ . An instantaneous reverse current jump occurs at  $t = T_1$  which here is avoided by minimizing the charge  $q_1$  by setting  $\delta \rightarrow 0$ .

making  $q_1 \rightarrow 0$ . In (2)  $q_0 = qAdp_1$  represents the variable remaining after  $\delta \rightarrow 0$ .

$$i_M(t) = \frac{q_0 - q_2}{T_{12}} \text{ where } T_{12} = \frac{d^2}{4D_a} \quad (2)$$

Here the term  $T_{12}$  represents the approximate diffusion transit time across the region  $q_2$ . The charge control continuity equation for  $q_2$  is

$$0 = \frac{dq_2}{dt} + \frac{q_2}{\tau} - \frac{q_0 - q_2}{2T_{12}} \quad (3)$$

The first term represents charge variation with respect to time, the second, recombination with lifetime  $\tau$ , and the third, diffusion of charge from the  $p^+i$  junction into  $q_2$ . Finally, the variable  $q_0$  which represents the injected charge level at the junction is related to the junction voltage  $\nu_E$  developed from the standard Law of Junction as follows:

$$q_0 = I_{S0}\tau \left[ \exp\left(\frac{\nu_E}{V_T}\right) - 1 \right] \quad (4)$$

Here  $I_{S0}$  represents the diode saturation current constant,  $V_T$  is the thermal voltage. Equations (2), (3), and (4) are the complete set of equations for this lumped charge model which includes reverse recovery.

Under reverse bias, the parameter  $T_{12}$  does not vary as the depletion width changes, the base contraction with increase of reverse blocking voltage is omitted in the model. Thus, diode reverse recovery in this model is independent of reverse bias voltage. Further information on this reverse recovery model is given in [5].

### B. Forward Recovery

Forward recovery occurs when a diode switches rapidly from its off-state to its on-state. During the transient, a high forward voltage builds up across the diode because of initial low conductivity in the  $i$ -region. As the injected carrier concentration increases, the voltage across the  $i$ -region soon decreases to the normal steady state diode forward drop. In the model, the injected carrier concentration is determined by the magnitude of  $q_2$  according to the following equation for carrier conduction by drift.

$$i = qA\mu(p_2 + p_{M0})\frac{\nu_M}{d} = \mu(q_2 + q_{M0})\frac{\nu_M}{d^2} = \frac{(q_2 + q_{M0})\nu_M}{4T_{12}V_T} \quad (5)$$

Here  $i$  is the total current through the  $i$ -region,  $\nu_M$  is the voltage across half of the  $i$ -region,  $\mu$  is the ambipolar mobility, and  $q_{M0} = qAdp_{M0}$  is the conduction charge due to  $i$ -region background doping  $p_{M0}$ . To make (5) more meaningful for application engineers,  $q_{M0}$  is replaced by the initial resistance  $R_{M0}$  in the  $i$ -region, using  $q_{M0} = 2V_T T_{12}/R_{M0}$ . Thus (5) becomes

$$\nu_M = \frac{2V_T T_{12} R_{M0} i}{q_2 R_{M0} + 2V_T T_{12}} \quad (6)$$

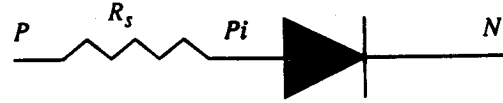


Fig. 3. Contact series resistor of the diode.

### C. Emitter Recombination

Under very high current level, the carrier recombination due to injection into the heavily doped  $p^+$  and  $n^+$  emitter regions (end regions in Fig. 2) becomes significant and must also be included [6]. The following expression is added to include this effect.

$$i_E = \frac{(n_p - n_{p0})qAL_p}{\tau_p} = I_{SE} \left[ \exp\left(\frac{2\nu_E}{V_T}\right) - 1 \right] \quad (7)$$

Here,  $i_E$  is the end region recombination current,  $n_p$  is the injected electron concentration in the  $P^+$  region,  $n_{p0}$  is the initial electron concentration,  $L_p$  is the electron diffusion length, and  $\tau_p$  is the carrier lifetime which is much smaller than that in the  $i$ -region. The constant  $I_{SE}$  is derived in the following manner. During high level injection the electron and hole concentrations are equal ( $n_1 = p_1$ ) in the  $i$ -region. The end region carrier concentrations  $n_p, p_p$  in Fig. 2 can be expressed as

$$n_p = n_1 \exp\left(-\frac{\phi_B - \nu_E}{V_T}\right) \quad (8)$$

where,  $\phi_B$  is the built-in potential. Replace  $n_1$  in (8) by the  $p_1$  expression acquired from

$$p_p = p_1 \exp\left(\frac{\phi_B - \nu_E}{V_T}\right) = N_A \quad (9)$$

and we obtain (10) for  $n_p$ . Insert  $n_p$  into (7) to obtain  $i_E$  as a function of  $\nu_E$ . The remaining constants can be represented by  $I_{SE}$  as given in (11).

$$n_p = N_A \exp\left(\frac{-2(\phi_B - \nu_E)}{V_T}\right) = N_A \exp\left(\frac{-2\phi_B}{V_T}\right) \exp\left(\frac{2\nu_E}{V_T}\right) \quad (10)$$

$$I_{SE} = \frac{qAL_p N_A}{\tau_p} \exp\left(-\frac{2\phi_B}{V_T}\right) \quad (11)$$

Normally,  $I_{SE}$  is many orders of magnitude smaller than  $I_{S0}$ , because  $i_E$  becomes a major part of the total current component only at very high currents. To make  $i_E = 0$  when  $\nu_E = 0$ , the "-1" term is added in (7).

### D. Complete Model

To complete the model equations, contact resistance and junction capacitance also must be included. This resistance is represented by an internal resistor  $R_s$  placed in series as shown in Fig. 3.

The conventional SPICE junction capacitance model [1] also needs to be added. Since the total p-n junction voltage is  $2\nu_E$ , for  $2\nu_E$ , less than  $\phi_B/2$ , (12) is used:

$$C_j = \frac{C_{j0}}{\left(1 - \frac{2\nu_E}{\phi_B}\right)^m} \quad (12)$$

Here,  $C_{j0}$  is the zero-biased junction capacitance. When the junction voltage  $2\nu_E$ , is greater than  $\phi_B/2$  the capacitance increases linearly with slope equal to that at  $2\nu_E = \phi_B/2$  for which (13) is employed.

$$C_j = \frac{m}{\phi_B} \frac{C_{j0}(2\nu_E)}{\left(\frac{1}{2}\right)^{m+1}} - (m-1) \frac{C_{j0}}{\left(\frac{1}{2}\right)^m} \quad (13)$$

The total stored charge  $q_j$  in the capacitor is

$$q_j = \int C_j d(2\nu_E) \quad (14)$$

Finally, three substitutions enable the complete set of model equations to be collected together in a simple and consistent form. The substitutions are:  $q_E = 2q_0$ ,  $q_M = 2q_2$ ,  $T_M = 2T_{12}$  and  $I_S = 2I_{S0}$ .

$$i_M = \frac{q_E - q_M}{T_M} \quad (15)$$

$$0 = \frac{dq_M}{dt} + \frac{q_M}{\tau} - \frac{q_E - q_M}{T_M} \quad (16)$$

$$q_E = I_S \tau \left[ \exp\left(\frac{\nu_E}{V_T}\right) - 1 \right] \quad (17)$$

$$\nu_M = \frac{V_T T_M R_{M0} i}{q_M R_{M0} + V_T T_M} \quad (18)$$

$$i_E = I_{SE} \left[ \exp\left(\frac{2\nu_E}{V_T}\right) - 1 \right] \quad (19)$$

$$\nu = 2\nu_E + 2\nu_M + R_s i \quad (20)$$

$$i = i_E + i_M + \frac{dq_j}{dt} \quad (21)$$

The capacitance  $C_j$  is connected across the  $2\nu_E$  term in (20).

### III. MODEL DEMONSTRATION AND DISCUSSION

Equations (15) to (21) were installed on the Saber simulator using the MAST modeling language. For simplicity, the parasitic elements are not included in the model. The model should also work in other analog circuit simulators which provide for insertion of mathematical equations. Some sample simulation results are presented here.

Fig. 4 shows the reverse recovery waveforms with the same lifetime  $\tau$  but two different values for the transit time  $T_M$ . The larger  $T_M$ , the more slowly the stored charges are removed from the base region. This usually corresponds to a wider base, higher breakdown voltage diode.

Sample forward recovery voltage waveforms corresponding to two different  $R_{M0}$  values are shown in Fig. 5. Diode initial low conductivity causes the high forward voltage drop at the beginning of the diode turn-on transient. The peak voltage depends on  $T_M$ ,  $\tau$ , and  $R_{M0}$ .

An examination of the forward bias static  $i$ - $v$  plot allows one to see more detailed information on the current components,

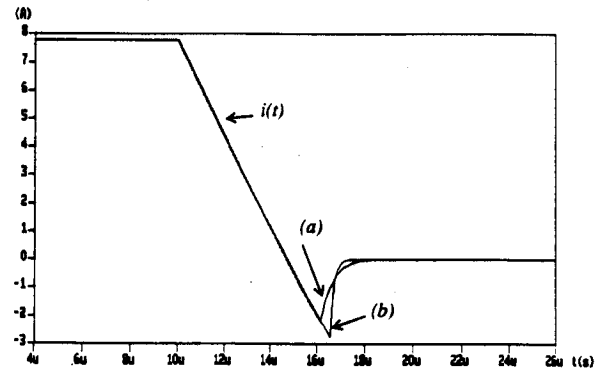


Fig. 4. Two reverse recovery waveforms with  $\tau = 1\mu s$ . (a)  $T_M = 1\mu s$ . (b)  $T_M = 0.2\mu s$ .

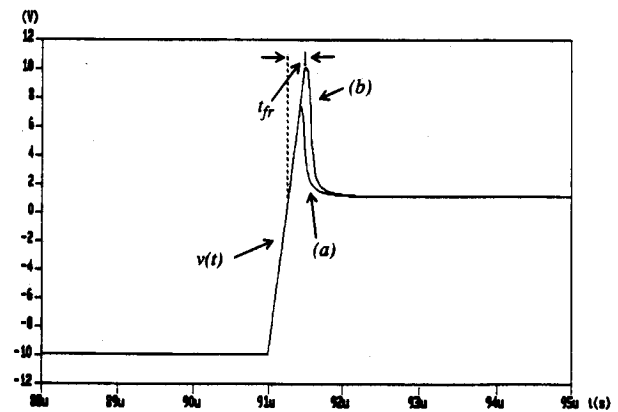


Fig. 5. Forward recovery voltage waveforms with (a)  $R_{M0} = 200\Omega$  (b)  $R_{M0} = 500\Omega$ ;  $T_M = 1\mu s$  and  $\tau = 5\mu s$  for both cases. The  $t_{fr}$  is shown for (b) only.

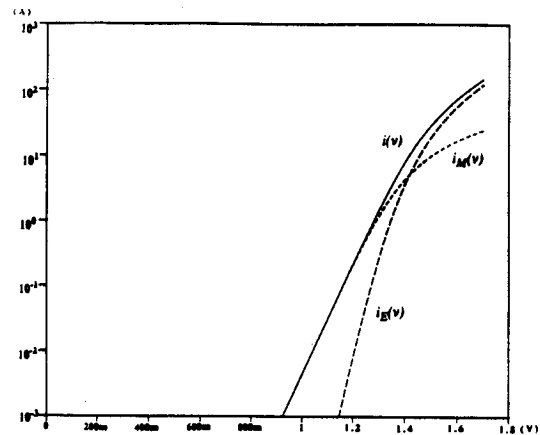


Fig. 6. Diode forward  $i$ - $v$  characteristic showing  $i(v)$  compared with internal current components  $i_E(v)$  and  $i_M(v)$ . ( $I_S = 10^{-10} A$ ,  $I_{SE} = 5 \times 10^{-22} A$ ,  $R_{M0} = 0$  and  $T_M = \tau = 2\mu s$ .)

$i_E$  and  $i_M$ , and the total current  $i$ . Fig. 6 is a semilog plot of these currents versus forward voltage where the model parameters are chosen to make  $i_E = i_M = 10 A$  (at  $i = 20 A$ ). Note, that at low current levels,  $i_M$  dominates the total current  $i$ ; but at current levels above 30 A, the end region emitter recombination current  $i_E$  becomes the dominant current component.

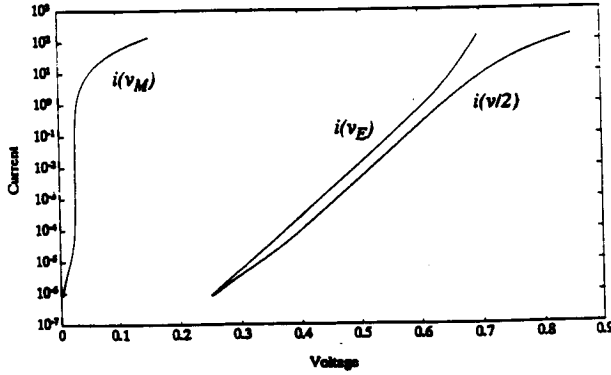


Fig. 7. Diode forward  $i$ - $v$  characteristic showing  $i(v/2)$  compared with  $i(v_E)$  and  $i(v_M)$ . The same parameters are used as in Fig. 6.

Fig. 7 is again a static  $i$ - $v$  plot under the same conditions as Fig. 6, but here the internal voltage components  $v_E, v_M$  are compared with half of the diode voltage  $v/2 = v_E + v_M$ . With the current less than 10 A, the  $i - v_E$  curve is a straight line since  $v_M$  is a small constant and  $\ln(i) \propto v_E$ . When the current is greater than 10 A, the slope increases and  $\ln(i) \propto 2v_E$ . However,  $v_M$  which is a constant at low currents from 10  $\mu$ A to 10 A, now starts increasing dramatically above 10 A due to the emitter recombination effect. Here, the injected carrier concentration in the  $i$ -region fails to increase as fast as the total current, which causes  $v_M$  to rapidly increase. The rapid increase in the external terminal voltage  $v$  above  $i = 10$  A is due to the increase in  $v_M$ .

#### IV. DETERMINATION OF MODEL PARAMETERS

Nine model parameters  $\tau, T_M, I_S, R_{M0}, I_{SE}, R_s, C_{j0}, \phi_B, m$ , need to be determined of which only three are new:  $T_M, R_{M0}$ , and  $I_{SE}$ ; the others are identical to the standard parameters used in the generic SPICE diode model.

1) The parameters  $\tau$  and  $T_M$  can be determined from a diode turn-off current waveform such as the typical inductive load waveform shown in Fig. 1. Three measurements are needed: the slope of the linear ramp for  $0 < t < T_1$ , the maximum reverse current  $I_{RM}$ , and the reverse recovery time constant  $\tau_{rr}$  from the exponential curve for  $t > T_1$ . From these measurements, one can easily calculate  $\tau$  and  $T_M$  using the parameter determination procedure provided in [5].

2) The parameter  $I_S$  is similar to the diode saturation current  $I_S$  used in the SPICE model. Under the static low current condition,  $i_M \gg i_E$  and  $q_M \gg V_T T_M / R_{M0}$ , from (15), (16), (18), and (20), we can derive the following equation to determine  $I_S$  from measured  $i$  and  $v$ .

$$I_S = \frac{(1 + \frac{T_M}{\tau})i}{\exp\left(\frac{v}{2V_T} - \frac{T_M}{\tau}\right)} \quad (22)$$

3) The forward recovery waveform shown in Fig. 5 can be estimated from the following equation:

$$\begin{aligned} v(t) - 2v_E(t) &= 2v_M(t) \\ &= \frac{2V_T T_M R_{M0} a t}{R_{M0} a \tau \left[ t - \tau \left( 1 - e^{-\frac{t}{\tau}} \right) \right] + V_T T_M} \end{aligned} \quad (23)$$

This equation is derived from (18) assuming the current increases linearly with time as  $i(t) = at$  where  $a$  is the constant rate of current rise. The charge  $q_M$  in (18) is replaced by  $q_M(t)$  determined by solving the differential equation (15) and (16) for  $i_M(t) = i(t) = at$  with the boundary condition  $q_M(t=0) = 0$ . Time  $t$  is zero when  $v_M(t) = 0$ . Using (23), parameter  $R_{M0}$  can be calculated from the initial slopes of the  $v(t)$  and  $i(t)$  waveforms.

$$R_{M0} = \frac{v - 2v_E}{2at} = \frac{1}{2} \frac{dv}{di} \quad (24)$$

The time  $t_{fr}$  of the peak forward recovery voltage shown in Fig. 5 can be determined by setting the derivative of (23) to zero, obtaining for  $t_{fr} \ll \tau$ :

$$t_{fr} = \left( \frac{2V_T T_M}{R_{M0} a} \right)^{\frac{1}{2}} \quad (25)$$

Thus, (25) represents an alternate way to extract  $T_M$ . Setting the parameter  $R_{M0}$  to zero eliminates both forward recovery and the increase in forward voltage drop at high currents due to emitter recombination. Thus, a finite value for  $R_{M0}$  is still recommended even if forward recovery performance is not of interest.

4) The parameters  $R_s$  and  $I_{SE}$  should be selected so as to best match the measured high current  $i - v$  characteristic.

5) The capacitance parameters  $C_{j0}, m$ , and  $\phi_B$  are determined from a standard capacitance-voltage plot in the conventional manner.

#### V. CONCLUSION

This p-i-n diode model includes complete forward and reverse recovery as well as the high current effects caused by emitter recombination. A major feature of the model is that the same equations are valid through all regions of operation. Except for the capacitance equation, no conditional statements are needed to define regions over which specific equations are valid. The model is simple and practical and should be considered as a new standard diode model for circuit simulation.

A similar modeling approach also can be applied to other conductivity modulated devices, including power devices such as SCR's, GTO's, BJT's, and IGBT's.

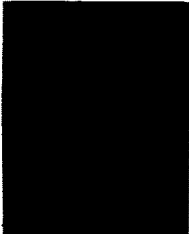
#### ACKNOWLEDGMENT

The authors would like to thank Dr. B. E. Danielsson of ABB and A. Persson from the Royal Institute of Technology in Sweden for their useful discussions and many suggestions in building this model.

#### REFERENCES

- [1] P. Antognetti and G. Massobrio, *Semiconductor Device Modeling with SPICE*. New York: McGraw-Hill, 1988.
- [2] Y.-C. Liang and V.J. Gosbell, "Diode forward and reverse recovery model for power electronic SPICE simulations," *IEEE Trans. Power Electron.*, vol. 5, pp. 346-356, July 1990.
- [3] B.E. Danielsson, "Studies of turn-off effects in power semiconductor devices," *Solid-State Electron.*, vol. 28, no. 4, pp. 375-391, 1985.
- [4] J. G. Linvill and J. F. Gibbons, *Transistors and Active Circuits*. New York: McGraw-Hill, 1961.

- [5] P. O. Lauritzen and C. L. Ma, "A simple diode model with reverse recovery," *IEEE Trans. Power Electron.*, vol. 6, pp. 188-191, Apr. 1991.
- [6] B. Jayant Baliga, *Modern Power Devices*. New York: Wiley, 1987, ch. 5.




**Cliff L. Ma (Ma Lie-wei)** was born in Beijing, China, on September 23, 1964. He studied at Tsinghua University in Beijing for four years, concentrating on semiconductor devices and physics. He received the B.S. degree from California State University, Fresno, in 1989 and the M.S. degree from the University of Washington in 1991, both in electrical engineering.

Currently, he is a Siemens Fellowship recipient at the University of Washington, Seattle, working toward the Ph.D. degree. His research interests

include semiconductor device modeling, circuit simulations and power electronics.

Mr. Ma is a member of Tau Beta Pi, Eta Kappa Nu, and the Golden Key National Honor Society.



**Peter O. Lauritzen (S'58-M'62-SM'88)** was born in Valparaiso, IN, on February 14, 1935. He received the B.S. degree in electrical engineering in 1956 from the California Institute of Technology, Pasadena and the M.S. and Ph.D. degrees in electrical engineering in 1958 and 1961, respectively, from Stanford University.

From 1961 to 1965 he worked on semiconductor device research and development at Fairchild Semiconductor Division, Palo Alto, CA. He has been on the electrical engineering faculty at the University of Washington, Seattle, since 1965, where his research activities have included semiconductor device noise, radiation effects, operation at cryogenic temperatures, and instrumentation. While on leave during 1979-1980 he was Engineering Manager of Avtech Corporation. Recently, he has worked on power electronic device modeling and protection. He is currently a Professor of electrical engineering.